

## Probing Shear-Band Initiation in Metallic Glasses

D. Klaumünzer,<sup>1</sup> A. Lazarev,<sup>2</sup> R. Maaß,<sup>1</sup> F. H. Dalla Torre,<sup>1</sup> A. Vinogradov,<sup>2,3,\*</sup> and J. F. Löffler<sup>1,†</sup>

<sup>1</sup>Laboratory of Metal Physics and Technology, Department of Materials, ETH Zurich, Wolfgang-Pauli-Strasse 10, 8093 Zurich, Switzerland

<sup>2</sup>Laboratory for Physics of Strength of Materials and Intelligent Diagnostic Systems, Togliatti State University, Togliatti 4455667, Russia

<sup>3</sup>Department of Intelligent Materials Engineering, Osaka City University, Osaka, 558-8585, Japan

(Received 30 June 2011; published 25 October 2011)

*In situ* acoustic emission monitoring is shown to capture the initiation of shear bands in metallic glasses. A model picture is inferred from stick-slip flow in granular media such that the origin of acoustic emission is attributed to a mechanism of structural dilatation. By employing a quantitative approach, the critical volume change associated with shear-band initiation in a metallic glass is estimated to be a few percent only. This result agrees with typical values of excess free volume found in the supercooled liquid regime near the glass transition temperature.

DOI: 10.1103/PhysRevLett.107.185502

PACS numbers: 62.20.F-, 43.40.Le, 47.20.Ft, 81.70.Bt

Despite different underlying length scales and bonding between individual constituents, a variety of disordered materials show remarkably similar flow behavior. These systems range from granular media and colloids to metallic glasses which are known to undergo localized deformation in shear bands as well as intermittent flow in a stick-slip fashion [1–3]. Both these common aspects of deformation, however, make it very hard to experimentally track any underlying microscopic flow mechanisms due to the associated strong localization of plastic strain in both space and time. This particularly applies to the case of metallic glasses in which shear bands are only a few hundreds of atoms thin [4] and believed to operate fast in less than a few milliseconds [5]. As a consequence, very fundamental aspects of plastic flow remain unresolved for metallic glasses at the atomic scale—much in contrast to crystalline metals. Unveiling the physics of plastic deformation hence relies on a detailed understanding of the origin and characteristics of shear bands.

As in any ordered or disordered material prone to exhibiting shear bands, the origin of flow localization is a feedback situation in which the onset of plastic deformation in a local region is accompanied by a softening mechanism which acts to preferentially concentrate further strain in the exact same location. The true cause of this softening may be manifold and induced by strain, strain rate, or local temperature [6]. For metallic glasses, it is believed to be directly associated with the atomic-scale flow processes which generate structural disordering [7,8] as revealed by preferential etching at shear bands [9]. This change in structure is most prominently attributed to local volume dilatation as shown, for example, in recent positron annihilation experiments [10] and is analogous to the deformation behavior of granular media [11]. In addition to this flow-induced effect, the possibility of thermal softening within shear bands has been investigated [12–14]. As

also confirmed in recent studies [15,16], however, the general conclusion drawn is that temperature rises may be only a consequence of severe flow localization but not its cause, and the primary origin of shear banding is indeed flow-induced.

While considerable attention has been paid to clarifying the origin of flow localization in metallic glasses, quantifying the degree of softening and dilatation within shear bands consistently by experiments remains an issue yet to be resolved. Very early attempts were done, on the one hand, by direct structural imaging of shear bands using transmission electron microscopy (TEM) [4] and, on the other hand, by detecting changes in crystallization shrinkage [17,18] or density [19] in severely deformed specimens. However, all of these studies remained somehow dissatisfying in their results for several reasons. Most importantly, very large estimates of volume expansion typically ranging between 10% and 20% were obtained, suggesting unrealistically strong softening. Additionally, the measurements were done *ex situ* after the removal of load, and the final results were often dependent on the overall level of strain imparted. In an attempt to explain these observations, the volume change estimated was attributed to remnants of that accumulated as a function of strain during shear, which was argued not to be accommodated at the atomic scale but coalesced in the form of nanovoids. This was also observed in the TEM study by Donovan and Stobbs [4] and later confirmed in Ref. [20]. In this respect, the above studies could not address the key question of primary scientific interest as to the critical degree of softening that is required to induce flow localization in metallic glasses.

It is clear that resolving this issue requires an experimental technique of sufficient spatial and time resolution to directly capture the fast and collective atomic-scale processes leading to softening and flow localization, i.e., the

birth of a shear band. In this work, we will show that *in situ* acoustic emission (AE) monitoring possesses the means to achieve this. We will thus demonstrate that AE activity is a precursor to shear-band propagation during serrated flow, which we therefore associate with shear-band initiation. We will draw an analogy to the stick-slip behavior of granular media, attributing shear-band initiation in the metallic glass to a softening mechanism by structural dilatation. By applying a quantitative methodology, the degree of dilatation will be estimated from the AE signal and shown to be comparable to a structural state similar to the supercooled liquid regime.

Cylindrical, amorphous rods of  $\text{Zr}_{52.5}\text{Ti}_5\text{Cu}_{17.9}\text{Ni}_{14.6}\text{Al}_{10}$  (Vit105) of 3 mm in diameter were prepared by suction casting in water-cooled Cu molds and subsequently cut into samples of 5 mm in length. Prior to compression testing, the upper and lower faces were polished to ensure proper alignment between the compression platens. A broadband AE sensor (MSAE-1300WB by Microsensors AE Ltd., Russia) with a multiple resonance frequency response between 50 and 1300 kHz was placed in a cavity in the lower platen coaxially aligned with the sample and covered by a protective tungsten-carbide plate. Compression tests were performed at strain rates of  $10^{-3}$ – $10^{-2}$   $\text{s}^{-1}$ . Load was measured by using a piezoelectric load cell as in Ref. [21–24]. A high acquisition rate of 10 kHz was chosen for the load signal recorded by an analogue-to-digital converter, while a continuous AE-stream was sampled at 2 MHz by using a high resolution 18 bit PCI-2 AE board (Physical Acoustic Corporation, USA). Both devices were synchronized to allow the time-resolved load data and AE stream to be superimposed on the time axis at high accuracy ( $\ll 1$  ms).

Figure 1(a) shows an overview of the stress-time curve and corresponding AE stream. Typical serrations are observed in the stress signal, indicative of an intermittent, stick-slip mechanism of shear-band operation with

repeated cycles of initiation, propagation, and arrest [24]. Comparing the acoustic emission signal to the features in the stress-time curve reveals a clear correlation between the occurrence of serrations and enhanced AE activity, as reported in preliminary studies [25,26]. Now exploiting the benefits of a high time resolution in stress paired with the synchronized AE stream demonstrates a clear time sequence of events. Figure 1(b) focuses on a single stress drop and the corresponding AE burst. The AE transient appears as a precursor to the stress drop and approximately aligns with peak stress. Bearing in mind that the stress drop is a natural system response to the propagation of a fully developed shear band [27], we can conclude that AE captures the preceding mechanism which we attribute to the birth of a shear band, i.e., shear-band initiation. By taking the rise time to be a measure of the duration of operation of the AE-source mechanism and attributing the decaying signal tail solely to vibrations and reflections within the sensor [see the inset in Fig. 1(b)], it is interesting to note that the initiation stage occurs within tens of microseconds, while shear-band propagation is much slower with associated durations of the order of a few milliseconds for ambient temperature [22,23]. Additionally, such a short duration of the AE source confirms that the sensor operates within the correct frequency range.

With evidence of an experimental technique capable of capturing shear-band initiation in metallic glasses, it is now of interest to characterize this stage in further detail. A potential underlying microscopic picture can be postulated by drawing an analogy to the intermittent flow behavior of granular media. The benefit of granular media is that particle rearrangements are sufficiently slow and coarse such that they can be followed *in situ* during shear [28], as this cannot be done for metallic glasses at the atomic level. In this context, the studies by Nasuno *et al.* [29] as well as Sundaram, Goodman, and Wang [30] are particularly valuable to this work as they successfully correlate

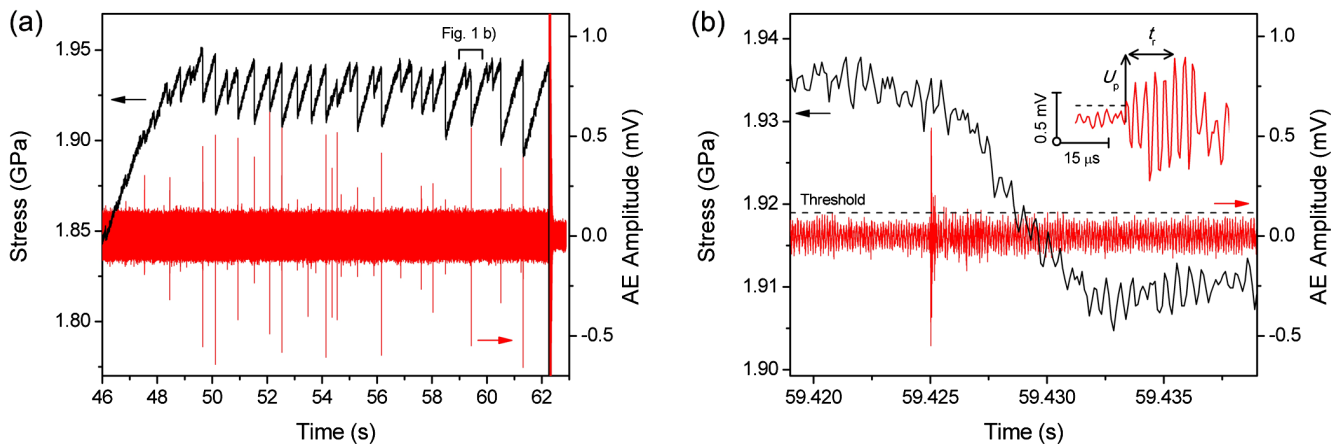


FIG. 1 (color online). (a) Time-resolved stress data and AE stream showing serrations and AE bursts to coincide. (b) Focus on a single load drop with AE activity as a precursor. Inset in (b): Magnification of the AE burst showing rise time  $t_r$ , measured from the first crossing of the threshold level to peak amplitude  $U_p$  within an error of  $\pm 5$   $\mu\text{s}$ .

time-resolved structural information as apparent from density changes to the intermittent slip dynamics and serrated flow behavior of model granular systems subjected to shear. Despite a different experimental approach, the two studies agree in the fact that an increase in volume (dilatation) precedes slip events. In analogy to the occurrence of the AE signal [see Fig. 1(b)], a maximum in both volume expansion and rate of dilatation is reached near or just after peak load, i.e., prior to the system attaining its maximum propagation velocity as reflected in load drops. We propose to adopt a qualitatively similar scenario for the case of the metallic glass with dilatation initiating and preceding localized plastic flow. We therefore attribute the AE signal to a collective atomic-scale mechanism that induces a local volume expansion across the shear plane during shear-band initiation.

Following from this, the next step in our analysis is a quantitative assessment of AE parameters with the aim to estimate the associated degree of dilatation during the initiation stage. Relating the AE wave detected at the sample surface to the triggering changes in local stress fields within the bulk is a mathematically formidable task as first outlined by Simmons and Clough [31] using a Green's function formalism. Based on this approach, Scruby, Baldwin, and Stacey [32] have proposed a simplifying method to associate the measurable AE parameters to the properties of the source. Their analysis is essentially based on reducing the AE source to a point, representing source forces as dipoles in two dimensions, and approximating the sample geometry by an infinite body. These assumptions make the mathematics analytically tractable. An expression can therefore be derived relating the measured normal surface displacement  $u(t)$  at the radial sensor position  $(r, \theta)$  to the time derivative of the source dipole tensor  $\dot{D}_{ij}$ , with the indices  $i$  and  $j$  referring to the directions of the forces and their separation, respectively:

$$u(t) = \frac{(\dot{D}_{11}\sin^2\theta + \dot{D}_{33}\cos^2\theta + 2\dot{D}_{13}\sin\theta\cos\theta)R_p}{4\pi(\lambda + 2\mu)c_1r}, \quad (1)$$

where  $\lambda$  is Lamé's parameter,  $\mu$  is the shear modulus, and  $c_1$  is the compression wave speed. The factor  $R_p$  takes into account reflection and mode conversion of the incident compression wave at the surface and is given by

$$R_p = \frac{2k^2\cos\theta'(k^2 - 2\sin^2\theta')}{(k^2 - 2\sin^2\theta')^2 + 4\sin^2\theta'(1 - \sin^2\theta')^{0.5}(k^2 - \sin^2\theta')^{0.5}}, \quad (2)$$

where  $\theta'$  is the angle between the incident wave and surface normal and  $k$  is the ratio between compression and shear wave speeds  $c_1$  and  $c_2$ .

The above approach is adapted to the specific testing geometry used in this study as shown in Fig. 2. The source dipole components  $D_{11}$  and  $D_{33}$  are assumed to be parallel and perpendicular to the shear band respectively. It follows that with a sensor placed at the epicenter below the sample,

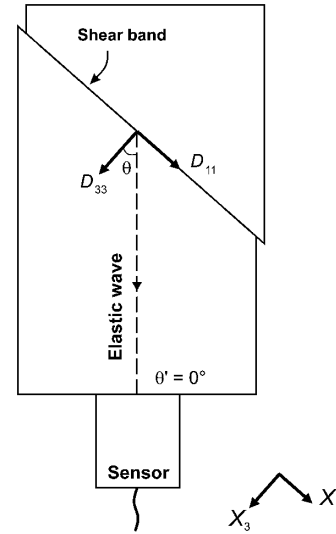


FIG. 2. Simplified AE setup with the AE source (shear band) oriented at  $45^\circ$  relative to the sensor.

$\theta$  equates to  $45^\circ$ ,  $\theta'$  is equal to  $0^\circ$ , and  $r$  can be taken as half of the specimen length  $l$ . Additionally, for a pure dilatation source,  $D_{13} = D_{31} = 0$  and  $D_{11} = D_{33} = \delta V(\lambda + 2/3\mu)$ , where  $\delta V$  is the volume change [32]. From the above, Eq. (1) reduces to

$$u(t) = \frac{\dot{D}_{11}R_p}{2\pi(\lambda + 2\mu)c_1l} = \delta\dot{V}\frac{R_p(\lambda + 2/3\mu)}{2\pi(\lambda + 2\mu)c_1l} \equiv C\delta\dot{V}; \quad (3)$$

i.e., the surface displacement is proportional to the dynamics of the dilatation source as given by the rate of volume change  $\delta\dot{V}$  and the constant  $C$ . In this study, we assume the AE source to be of collective character and composed of multiple, overlapping elementary source events of the form of Eq. (3). The collective source is active during a time interval defined by the rise time  $t_r$  [see the inset in Fig. 1(b)]. During this time, the shear-band initiation process occurs which requires a sufficiently large number of atomic-scale events to span the entire shear plane on completion. We further assume that the collective AE source expands progressively at an increasing rate towards a critical level  $\delta V_t$  beyond which the band begins to propagate. In approximation, the accelerating dynamics of the collective source is reflected in the increasing upper amplitude level during the AE burst [inset in Fig. 1(b)], which may be fitted as a linear function in time between the first threshold crossing at  $t'$  and the peak amplitude  $U_p$  at  $t' + t_r$ . As apparent from Eq. (3), the total volume change associated with the shear-band initiation process is therefore given by integration of that linear function with respect to time or, in other words, by the area of a triangular envelope outlining the ascending, upper half of the AE burst:

$$\delta V_t = \frac{1}{C} \int_{t'}^{t'+t_r} u(t)dt \approx \frac{1}{2C} t_r U_p k_f, \quad (4)$$

where  $k_f$  is the sensor calibration factor used to convert the measured amplitude (in volts) into units of surface displacement (meters). The above procedure accounts for the fact that the oscillatory form of the AE signal is due to resonances within the sensor and bears little resemblance to the actual source mechanism. Only broadband sensors of perfectly flat frequency response would possess the capacity of reproducing the fine details of temporal changes in the dynamics of the AE source but typically at a substantial loss of sensitivity. The use of the more sensitive, multiple-frequency resonance sensor in this study limits the true source parameters to rise time and calibrated peak amplitude (see Ref. [33] for details on the calibration procedure) but permits a justified estimate of the total volume change on the basis of Eq. (4).

The total volume change  $\delta V_t$  is normalized with respect to the volume  $V$  of a fully developed shear band spanning the full cross section of the sample to determine the degree of shear-band dilatation  $\delta V/V$ . A shear-band thickness of 15 nm is assumed in calculating  $V$ , representing a reasonable mean of the range of values typically reported [4,34]. Figure 3 shows a histogram of  $\delta V/V$  determined from 76 AE transients with input parameters summarized in Table I. The values span a range from just below 0.5% to about 8% with a median of 2%. More importantly, roughly two-thirds of all values lie between 0.5%–3%. It is remarked that these estimates of shear-band dilatation are consistently smaller than those reported in any earlier study [4,17–19].

This result raises two immediate questions: (i) Why are volume changes estimated from AE measurements smaller than those detected by microscopy, direct density measurements, or dilatometry [4,17–19]? (ii) How realistic are these smaller values? In answering the first question,

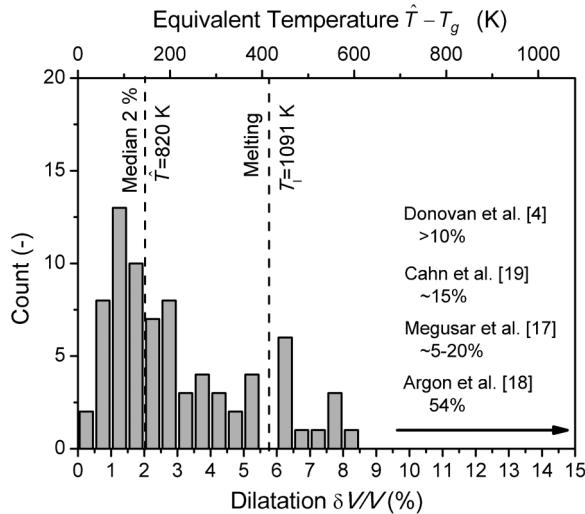


FIG. 3. Histogram of values of shear-band dilatation calculated from 76 AE bursts. Associated apparent equivalent temperatures from Eq. (6) reveal that most values lie in the supercooled liquid regime close to the glass transition.

TABLE I. Input parameters used to calculate values of shear-band dilatation according to Eqs. (3) and (4) as well as mean values of peak amplitude  $\bar{U}_p$  and rise time  $\bar{t}_r$ .

Parameter	Input value	Ref.
$\theta$	45°	Figure 2
$\theta'$	0°	Figure 2
$R_p$	2	Equation (2)
$r$	2.5 mm ( $l/2$ )	...
$\mu$	32.3 GPa	[35]
$E$	88.6 GPa	[35]
$\lambda$	91.9 GPa	From $E$ and $\mu$
$c_1$	$3.62 \times 10^3$ m/s	From $E$
$c_2$	$2.19 \times 10^3$ m/s	From $\mu$
$k_f$	$2.0 \times 10^{-11}$ m/mV	...
$\bar{U}_p$	0.28 mV	...
$\bar{t}_r$	25 $\mu$ s	...
$V$	$1.5 \times 10^{-13}$ m <sup>3</sup>	...

it is important to stress the conceptual differences between this work and the original studies. The major drawbacks of the first experimental attempts to measure shear-band dilatation were that they represented *ex situ* measurements, bore an unresolved influence of strain, and most importantly were attributed to excess volume accommodated in nanovoids, i.e., at a scale coarser than the atomic level. In contrast, offering a markedly different experimental perspective, AE monitoring in this work captures processes in real time at any value of strain that, in addition, can be attributed to the collective atomic-scale mechanisms governing the onset of yielding. In other words, this AE study provides an *in situ* estimate of the atomic-scale volume change required to cause the critically necessary local softening for initiating a shear band.

As the original studies [4,17–19] cannot serve as a comparison, validation of the given results needs to be sought elsewhere in addressing question (ii). This can be done by comparing the volume changes assessed by AE to the free volume changes predicted as a function of temperature. The free volume content  $V_f$  of a metallic glass is believed to follow a temperature dependence of the form [36]

$$V_f(T) = V_0 + V_m(\alpha_l - \alpha_g)(T - T_g), \quad (5)$$

with  $T > T_g$ ,  $V_0$  representing the free volume content below the glass transition  $T_g$ , which is assumed to be constant,  $V_m$  being the molar volume, and  $\alpha_g$  and  $\alpha_l$  referring to the volume thermal expansion coefficients of the glass and the liquid, respectively. We can now define an apparent equivalent temperature which would yield the same increase in free volume  $\Delta V_f = V_f(\hat{T}) - V_0$  on heating to temperatures above  $T_g$  as the volume change  $\delta V$  detected by AE normalized with respect to the number of atoms within a shear band ( $V/V_m$ ):

$$\delta V \frac{V_m}{V} \equiv V_f(T) - V_0 = V_m(\alpha_l - \alpha_g)(\hat{T} - T_g) \quad \text{or}$$

$$\hat{T} - T_g = \frac{\delta V}{V} \frac{1}{(\alpha_l - \alpha_g)}. \quad (6)$$

The thermal expansion coefficients  $\alpha_g$  and  $\alpha_l$  can be calculated to be  $3.3 \times 10^{-5}$  and  $17.1 \times 10^{-5} \text{ K}^{-1}$ , respectively, from the data in Ref. [37] for a Zr-based glass of similar composition. Taking  $T_g$  to be equal to 675 K [38] allows for expressing the measured values of dilatation  $\delta V/V$  in terms of an equivalent temperature:  $\hat{T} - T_g$ . This is facilitated by the upper horizontal axis in Fig. 3. It is apparent that most of the data fits well within the supercooled liquid regime with a hypothetical upper limit corresponding to the liquidus temperature  $T_l$  (1091 K [38]). It is again clear that, with a median value of 2% dilatation corresponding to an equivalent temperature of 820 K ( $\hat{T} - T_g = 145 \text{ K}$ ), the weight of the distribution lies towards the lower end, i.e., close to the glass transition. It can therefore be concluded that the critical degree of dilatation associated with the onset of yielding is that resulting in a structural state and atomic mobility comparable to the supercooled liquid regime near the glass transition temperature. This result provides valuable experimental support of recent, mainly theoretical work in which yielding is proposed to bear a close resemblance to a stress-induced glass transition [39,40].

In conclusion, we have shown that AE monitoring of serrated flow in metallic glasses possesses the powerful means to capture the process of shear-band initiation. Inspired from a phenomenological analogy of the intermittent flow behavior of sheared granular media, we attribute this stage to a softening mechanism by local structural dilatation. A quantitative analysis of AE waveforms permits an *in situ* estimate of the critical volume change required to initiate localized plastic flow. The degree of dilatation within a shear band is found to be no more than a few percent, in agreement with typical values of excess free volume characteristic of the supercooled liquid regime close to the glass transition temperature.

Support by the Swiss National Science Foundation (SNF Grants No. 200020-120258 and No. 200020-135100) is gratefully acknowledged.

\*alexei.vino@gmail.com

†joerg.loeffler@mat.ethz.ch

- [1] S. Nasuno, A. Kudrolli, and J.P. Gollub, *Phys. Rev. Lett.* **79**, 949 (1997).
- [2] A. Lemaître, *Phys. Rev. Lett.* **89**, 195503 (2002).
- [3] P. Schall and M. van Hecke, *Annu. Rev. Fluid Mech.* **42**, 67 (2010).
- [4] P.E. Donovan and W.M. Stobbs, *Acta Metall.* **29**, 1419 (1981).
- [5] H. Neuhäuser, *Scr. Metall.* **12**, 471 (1978).
- [6] J.P. Poirier, *J. Struct. Geol.* **2**, 135 (1980).
- [7] F. Spaepen and D. Turnbull, *Scr. Metall.* **8**, 563 (1974).
- [8] F. Spaepen, *Acta Metall.* **25**, 407 (1977).
- [9] C.A. Pampillo, *Scr. Metall.* **6**, 915 (1972).
- [10] K.M. Flores, D. Suh, and R.H. Dauskardt, *J. Mater. Res.* **17**, 1153 (2002).
- [11] O. Reynolds, *Philos. Mag.* **20**, 469 (1885).
- [12] W.J. Wright, R.B. Schwarz, and W.D. Nix, *Mater. Sci. Eng. A* **319–321**, 229 (2001).
- [13] B. Yang *et al.*, *Appl. Phys. Lett.* **86**, 141904 (2005).
- [14] J.J. Lewandowski and A.L. Greer, *Nature Mater.* **5**, 15 (2006).
- [15] Y.Q. Cheng *et al.*, *Phys. Rev. B* **80**, 134115 (2009).
- [16] D.B. Miracle *et al.*, *Acta Mater.* **59**, 2831 (2011).
- [17] J. Megusar, A.S. Argon, and N.J. Grant, *Mater. Res. Soc. Symp. Proc.* **8**, 283 (1982).
- [18] A.S. Argon, J. Megusar, and N.J. Grant, *Scr. Metall.* **19**, 591 (1985).
- [19] R.W. Cahn *et al.*, *Mater. Res. Soc. Symp. Proc.* **28**, 241 (1984).
- [20] J. Li, Z.L. Wang, and T.C. Hufnagel, *Phys. Rev. B* **65**, 144201 (2002).
- [21] W.J. Wright *et al.*, *Acta Mater.* **57**, 4639 (2009).
- [22] D. Klaumünzer *et al.*, *Appl. Phys. Lett.* **96**, 061901 (2010).
- [23] R. Maaß, D. Klaumünzer, and J.F. Löffler, *Acta Mater.* **59**, 3205 (2011).
- [24] D. Klaumünzer, R. Maass, and J.F. Löffler, *J. Mater. Res.* **26**, 1453 (2011).
- [25] F.H. Dalla Torre *et al.*, *Acta Mater.* **58**, 3742 (2010).
- [26] A. Vinogradov, *Scr. Mater.* **63**, 89 (2010).
- [27] S.X. Song, X.L. Wang, and T.G. Nieh, *Scr. Mater.* **62**, 847 (2010).
- [28] P. Schall, D.A. Weitz, and F. Spaepen, *Science* **318**, 1895 (2007).
- [29] S. Nasuno *et al.*, *Phys. Rev. E* **58**, 2161 (1998).
- [30] P.N. Sundaram, R.E. Goodman, and C.-Y. Wang, *Geology* **4**, 108 (1976).
- [31] J.A. Simmons and R.B. Clough, in *Proceedings of the International Conference on Dislocation Modelling of Physical Systems, Gainesville, 1980*, edited by J.P. Hirth and M. Ashby (Pergamon, Oxford, 1981), p. 464.
- [32] C.B. Scruby, G.R. Baldwin, and K.A. Stacey, *Int. J. Fract.* **28**, 201 (1985).
- [33] S. Lazarev *et al.*, *J. Acoustic Emission* **27**, 212 (2009).
- [34] Y. Zhang and A.L. Greer, *Appl. Phys. Lett.* **89**, 071907 (2006).
- [35] B. Zan *et al.*, *Appl. Phys. Lett.* **81**, 4739 (2002).
- [36] M.H. Cohen and D. Turnbull, *J. Chem. Phys.* **31**, 1164 (1959).
- [37] N. Mattern *et al.*, *Mater. Sci. Eng. A* **375–377**, 351 (2004).
- [38] S.C. Glade *et al.*, *J. Appl. Phys.* **87**, 7242 (2000).
- [39] B. Yang, C.T. Liu, and T.G. Nieh, *Appl. Phys. Lett.* **88**, 221911 (2006).
- [40] P. Guan, M.W. Chen, and T. Egami, *Phys. Rev. Lett.* **104**, 205701 (2010).